

A Green's function approach to analysing the effects of random synaptic background activity in a model neural network

This article has been downloaded from IOPscience. Please scroll down to see the full text article.

1994 J. Phys. A: Math. Gen. 27 4097

(<http://iopscience.iop.org/0305-4470/27/12/017>)

View [the table of contents for this issue](#), or go to the [journal homepage](#) for more

Download details:

IP Address: 171.66.16.68

The article was downloaded on 01/06/2010 at 21:46

Please note that [terms and conditions apply](#).

A Green's function approach to analysing the effects of random synaptic background activity in a model neural network

Paul C Bressloff

Department of Mathematical Sciences, Loughborough University of Technology,
Loughborough, Leicestershire LE11 3TU, UK

Received 27 September 1993

Abstract. The effect of randomly distributed synaptic background activity on the states of self-sustained firing in a model neural network with shunting is investigated. Using mean field theory, the steady state of the network is expressed in terms of an ensemble-averaged single-neuron Green's function. This Green's function is shown to satisfy a matrix equation identical in form to that found in the tight-binding-alloy (TBA) model of excitations on a one-dimensional disordered lattice. The ensemble averaging is then performed using a coherent potential approximation (CPA) thus allowing the steady-state firing rate of the network to be determined. The firing rate is found to decrease as the mean level of background activity across the network is increased; a uniform background (zero variance) leads to a greater reduction than a randomly distributed one (non-zero variance).

1. Introduction

The change in the membrane potential of a neuron induced by a synaptic input depends on the size of the deviation of the membrane potential from some fixed resting potential. Recent studies have shown that if these so-called shunting effects are taken into account then (i) a nonlinear relationship can arise between the input current to the soma of a neuron and the incident rates of excitatory inputs synapsing on the dendritic tree of a neuron (Abbott 1991, Bressloff and Taylor 1993a, b) and (ii) the inclusion of background synaptic activity leads to a modification in the effective membrane potential time constant of a neuron (Bressloff and Taylor 1993b, Bressloff 1993).

The nonlinearity due to shunting produces a low-output firing rate in the presence of high levels of input excitation. Thus, if a network of such neurons is in a state of self-sustained firing corresponding, for example, to a dynamical fixed point in an attractor network (Amit 1989), then the neurons tend to fire well below their maximum rate. This is consistent with what is observed in certain cortical neurons, and provides a solution to the problem of high firing rates found in network models based on neurons whose input current varies linearly with synaptic inputs (no shunting). This latter problem has received considerable attention in the context of associative memory, where the self-sustained firing pattern is interpreted as a memory state (Amit and Treves 1989, Rubin and Sompolinsky 1989).

Modifications in the membrane potential time constant of a neuron due to synaptic background noise can also have important consequences since the time constant parametrizes the temporal evolution of the response of a neuron to an input. This has been explored from the viewpoint of temporal pattern processing elsewhere (Bressloff 1993, Bressloff and

Taylor 1993b). We note here that recent experiments indicate that variations in background synaptic activity can lead to a membrane time constant taking a range of values between 5 and 80 ms, (Bernander *et al* 1991, Rapp *et al* 1992).

In this paper, we analyse the effects of background synaptic activity on the state of self-sustained firing in a shunting network based on a compartmental model of a neuron. A compartmental model (Rall 1964, 1967) represents the electrical properties of the dendritic tree of a neuron by dividing the latter into sufficiently small regions or compartments such that spatial variation of electrical and physical properties within a region are negligible. For simplicity, we represent the dendritic tree as a one-dimensional chain of compartments. The background synaptic inputs are distributed randomly across the neurons of the network. Using mean field theory arguments (Abbott 1991), we show how the steady state of the network is determined by an ensemble-averaged single-neuron Green's function, which satisfies a matrix equation identical in form to that found in the tight-binding-alloy (TBA) model of excitations on a one-dimensional disordered lattice (Elliott *et al* 1974, Ziman 1979). Green's function techniques such as the coherent potential approximation (CPA) are then used to analyse the effects of statistical fluctuations arising from the distribution of synaptic background activity on the steady-state behaviour of the network. It is found that synaptic background activity leads to a reduction in the firing rate, which becomes more pronounced as the mean level of background activity across the network increases. Furthermore, a uniform background produces a greater reduction than a randomly distributed one.

The organization of the paper is as follows: the compartmental model is introduced in section 2, and the mean field analysis of a network with background noise is developed in section 3. The Green's function formalism of disordered lattices and its application to the study of the effects of background noise on network behaviour is presented in section 4.

2. Compartmental model neuron

Consider a compartmental model neuron that consists of a chain of $2M + 1$ dendritic compartments labelled $m = 1, \dots, \pm M$ together with a single somatic compartment. The passive membrane properties of each compartment m may be represented electrically in terms of an equivalent circuit consisting of a membrane leakage resistor R_m in parallel with a capacitor C_m , with the ground representing the extracellular medium (assumed to be an isopotential). The electrical potential V_m across the membrane is measured with respect to the resting potential, i.e. the potential when there is no current flowing across the membrane. The compartment is joined to its immediate neighbours in the chain by the junctional resistors $R_{m,m-1}$ and $R_{m,m+1}$ (figure 1). The time evolution of the membrane potential is determined by Kirchoff's law: for each compartment, the total current through the membrane is equal to the difference between the longitudinal currents entering and leaving that compartment. Thus,

$$C_m \frac{dV_m}{dt} = -\frac{V_m}{R_m} + \sum_{(n;m)} \frac{V_n - V_m}{R_{mn}} + u_m \quad (2.1)$$

where u_m represents the net external input current into the compartment, and $(n;m)$ indicates that the summation over n is restricted to immediate neighbours of m . Note that more complex dendritic geometries can be modelled by taking the compartments to lie on the

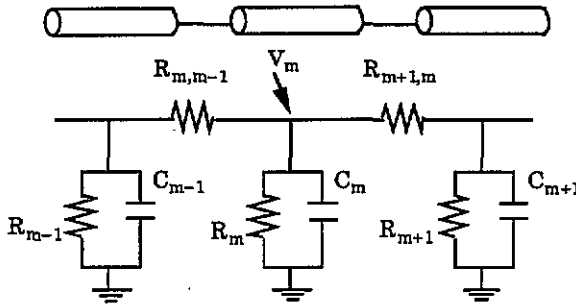


Figure 1. Equivalent circuit for a compartmental model of a chain of successive cylindrical segments of a passive dendritic membrane.

nodes of a tree and applying Kirchoff's law accordingly. However, for the purposes of this paper it will be sufficient to consider the simpler one-dimensional lattice.

A major simplification of the model is to view the soma as a point processor that is isopotential with the dendritic compartment nearest to it. The latter is chosen to be at the centre of the chain so that the membrane potential of the soma satisfies $V \equiv V_0$. (This choice allows us to ignore end effects in the large chain limit.) The neuron fires whenever the membrane potential at the soma exceeds some threshold h , and provided that the neuron is outside its absolute refractory period t_R . The effects of relative refractory period may be incorporated by introducing a time-dependent threshold of the form $h(\Delta t)$, where Δt is the time after emission of the last action potential, such that $h(\Delta t) = \infty$ for $0 < \Delta t \leq t_R$ and $h(\Delta t)$ is continuous and monotonically decreasing for $\Delta t > t_R$ (until the neuron fires again), e.g. $h(\Delta t) = h_0 + h_1 \exp(-\Delta t/\tau_a)$ for $\Delta t > t_R$ where $h_{0,1}$ and τ_a are constants. If $V(t)$ is slowly varying, then one can approximate the instantaneous firing rate $f(t)$ of the neuron by a sigmoid function,

$$f(t) = F(V(t)) = \frac{f_{\max}}{1 + e^{-g(V(t)-\kappa)}} \tag{2.2}$$

for some gain g and threshold κ . Equation (2.2) reflects the fact that the larger $V(t)$, the faster the decreasing threshold $h(\Delta t)$ is crossed from below and thus the greater the firing rate f . The maximum firing rate f_{\max} is determined by the absolute refractory period.

To complete the description of the model it is necessary to specify the form of the synaptic inputs. The crucial feature of such inputs as far as the development of this paper is concerned is that the changes in membrane potential V_n induced by a synaptic input depends on the size of the deviation of V_n from some fixed reversal potential. We shall refer to this as a *shunting effect*. If this is included, then the input current u_n of equation (2.1) becomes V_n -dependent. More specifically, let $\Delta g_{\alpha n}$ denote the increase in synaptic conductance induced by the arrival of action potentials at the α^{th} synapse of the n^{th} compartment with $\alpha = 1, \dots, N$. Ignoring voltage-dependent conductance changes arising from active processes, we shall take $\Delta g_{\alpha n}(t) = \epsilon_{\alpha n} x_{\alpha n}(t)$, where $x_{\alpha n}(t)$ is the arrival rate of action potentials at synapse (αn) and the constant $\epsilon_{\alpha n}$ is determined by factors such as the amount of neurotransmitter released in response to an action potential and the efficiency with which the neurotransmitters bind to receptors in the post-synaptic membrane. The total synaptic current u_m is then given by

$$u_m(t) = \sum_{\alpha=1}^N x_{\alpha m}(t) \epsilon_{\alpha m} (S_{\alpha m} - V_m(t)) + I_m(t) \tag{2.3}$$

where $S_{\alpha m}$ is the membrane reversal potential of synapse (αm). We have also included an external injection current $I_m(t)$.

Equations (2.1) and (2.3) may be combined to give a linear matrix equation of the form (Perkel *et al* 1981)

$$\frac{dV}{dt} = \hat{Q}(t)V(t) + U(t) \quad (2.4)$$

where $V = (V_{-M}, \dots, V_M)$,

$$\hat{Q}_{mn}(t) = Q_{mn} - \Gamma_m(t)\delta_{mn} \quad (2.5)$$

$$Q_{mn} = -\left(\frac{1}{\tau_m} + \sum_{\langle m':m \rangle} \frac{1}{\tau_{mm'}}\right)\delta_{mn} + \sum_{\langle m':m \rangle} \frac{\delta_{m'n}}{\tau_{mm'}} \quad (2.6)$$

$$\Gamma_m(t) = \sum_{\alpha} \frac{\epsilon_{\alpha m}}{C_m} x_{\alpha m}(t) \quad C_m U_m(t) = \sum_{\alpha} \epsilon_{\alpha m} S_{\alpha m} x_{\alpha m}(t) + I_m(t) \quad (2.7)$$

and $\tau_m = R_m C_m$, $\tau_{mm'} = R_{mm'} C_m$ are membrane time constants. We shall refer to $\Gamma_m(t)$ as a shunting term since it arises from the voltage-dependent contribution to the synaptic input u_m of equation (2.3). It is clear from equations (2.5) and (2.6) that one can interpret the shunting term as an input-dependent modification of the membrane time constant τ_m , i.e. $1/\tau_m \rightarrow 1/\tau_m + \Gamma_m(t)$. (Note that modifications in the membrane potential time constant by synaptic activity has recently been observed in a number of experiments (Bernander *et al* 1991, Rapp *et al* 1992).)

The solution of equation (2.4) under the initial condition $V(0) = 0$ may be expressed formally as

$$V(t) = \int_0^t dt' T \left[\exp \left(\int_{t'}^t \hat{Q}(t'') dt'' \right) \right] U(t') \quad (2.8)$$

where T denotes the time-ordering operator, i.e. $T(\hat{Q}(t)\hat{Q}(t')) = \hat{Q}(t)\hat{Q}(t')\theta(t-t') + \hat{Q}(t')\hat{Q}(t)\theta(t'-t)$ and $\theta(x) = 1$ for $x \geq 0$ and $\theta(x) = 0$ otherwise. In general, equation (2.8) is difficult to analyse. However, if the shunting term $\Gamma(t)$ is dropped from equation (2.5) then equation (2.8) reduces to

$$V_m(t) = \sum_n \int_0^t dt' \mathcal{G}_{mn}(t-t') U_n(t') \quad (2.9)$$

$$\mathcal{G}_{mn}(t) = [e^{tQ}]_{mn}. \quad (2.10)$$

We identify \mathcal{G}_{mn} as the membrane potential response function or Green's function of the dendritic chain. This is, $\mathcal{G}_{mn}(t-t')$ determines the membrane potential of compartment m at time t in response to a voltage-independent input current stimulation of compartment n at time t' . Note that in contrast to the time-ordered expression of equation (2.8), the Green's function only depends on the time difference $t-t'$.

The matrix Q defined in equation (2.6) has real, negative, non-degenerate eigenvalues λ_i reflecting the fact that it determines the time evolution of membrane potentials in a passive RC circuit, which is a dissipative system. Thus, \mathcal{G} has the general form

$$\mathcal{G}_{mn}(t) = \sum_i \exp(-t|\lambda_i|) B_{mn}^{(i)} \quad (2.11)$$

where the coefficients $B_{mn}^{(t)}$ can be determined using Sylvester's expansion theorem. A simple analytical expression can be derived for the Green's function $\mathcal{G}^{(0)}$ of an infinite, uniform chain using standard results from the theory of diffusion on a lattice (Bressloff and Taylor, 1993b). The uniformity condition is imposed by setting

$$R_m = R \quad C_m = C \quad R_{m,m+1} = R_{m+1,m} = R' \quad \tau = RC \quad \tau' = R'C \quad (2.12)$$

such that $\mathcal{G}_{mn}^{(0)}$ satisfies the differential equation

$$\frac{d\mathcal{G}_{mn}^{(0)}}{dt} = -\left(\frac{1}{\tau} + \frac{2}{\tau'}\right) \mathcal{G}_{mn}^{(0)}(t) + \frac{1}{\tau'}(\mathcal{G}_{m-1,n}^{(0)} + \mathcal{G}_{m+1,n}^{(0)}) \quad \mathcal{G}_{mn}^{(0)} = \delta_{mn}. \quad (2.13)$$

Equation (2.13) may be solved using Fourier method with $\mathcal{G}_{mn}^{(0)}$ depending only on the difference $|m - n|$. The result is

$$\mathcal{G}_{mn}^{(0)}(t) = \int_{-\pi}^{\pi} \frac{dk}{2\pi} e^{ik(m-n)} e^{-t\epsilon(k)} \quad (2.14)$$

where

$$\epsilon(k) = \frac{1}{\tau} + \frac{2}{\tau'}(1 - \cos k). \quad (2.15)$$

Equation (2.14) may be rewritten as $\mathcal{G}_{mn}^{(0)}(t) = e^{-t/\tau} I_{|m-n|}(2t/\tau')$, where I_p is the modified Bessel function of integer order. Note that we can also calculate $\mathcal{G}^{(0)}$ directly from equation (2.10) by setting $Q = Q^{(0)}$, where

$$Q_{mn}^{(0)} = -\left(\frac{1}{\tau} + \frac{2}{\tau'}\right) \delta_{mn} + \frac{1}{\tau'}(\delta_{m,n-1} + \delta_{m,n+1}) \quad (2.16)$$

expanding the matrix $e^{tQ^{(0)}}$ in powers of t , and using results from the theory of random walks on a lattice. This latter approach can be generalized to the case of more complex topologies associated with the dendritic tree (Bressloff and Taylor 1993c).

3. Shunting inhibition and synaptic background activity

When shunting effects are included in equation (2.1) the resulting solution (2.8) for the membrane potentials involves a time-ordered product that is difficult to analyse without further assumptions concerning the synaptic inputs. One major simplification is to take the rates of input stimulation to be constant. In particular, suppose that each compartment of a uniform chain consists of two groups of identical synapses, one excitatory and the other inhibitory. Equation (2.7) becomes

$$\begin{aligned} \Gamma_m &= c^{(e)} E_m + c^{(h)} H_m \\ U_m(t) &= c^{(e)} S^{(e)} E_m + c^{(h)} S^{(h)} H_m + I_m(t) \end{aligned} \quad (3.1)$$

where E_m and H_m are the constant rates of excitatory and inhibitory stimulation of the m th compartment, and $S^{(e,h)}$ are the corresponding reversal potentials with $S^{(e)} > 0$, $S^{(h)} \leq 0$. The constants $c^{(e,h)}$ are determined by the density and efficiency of synapses across a

compartment, and together with the reversal potentials are assumed to be site-independent. Since Γ_m and hence \hat{Q} are now time-independent, equation (2.8) reduces to

$$V_m(t) = \sum_n \int_0^t dt' \hat{G}_{mn}(t-t') U_n(t') \quad (3.2)$$

where

$$\hat{G}_{mn}(t) = \left[e^{t\hat{Q}} \right]_{mn} \quad \hat{Q}_{mn} = Q_{mn} - (c^{(e)} E_m + c^{(h)} H_m) \delta_{mn}. \quad (3.3)$$

Thus, in the presence of shunting, the membrane potential V_m in equation (2.10) is a nonlinear function of the constant excitatory and inhibitory inputs E_m and H_m . As pointed out previously (Abbott 1991, Bressloff and Taylor 1993a, b), this feature is important since a recurrent network of such neurons can operate in a regime of self-sustained firing in which the neurons are firing well below their maximum rate f_{\max} ; this is consistent with what is observed in real cortical systems. (Standard associative networks, on the other hand, consist of neurons whose membrane potential or activation state is linear in inputs, so that they tend to fire at their maximum rate (Amit 1989).)

To illustrate this point in more detail, we shall follow the discussion of Bressloff and Taylor (1993b) and determine the steady-state value V^∞ of the membrane potential at the soma in the case of the infinite uniform dendritic chain. We shall take the pattern of input stimulation to be in the form of non-recurrent lateral inhibition as illustrated in figure 2. That is, an input that excites the m th compartment also inhibits all other compartments in the chain. In particular, we choose a pattern of excitatory and inhibitory stimulation such that

$$E_0 = 0 \quad E_n = a_n E \quad \sum_n a_n = 1 \quad (3.4a)$$

$$H_m = \sum_{n \neq m} E_n. \quad (3.4b)$$

We have assumed that there is no direct stimulation of the soma ($E_0 = 0$) and that the relative distribution of excitation across the chain as specified by the a_n s is fixed. We have also set $c^{(e,h)} = 1$ for convenience. It then follows that the shunting term Γ_m of equation (3.1) becomes site-independent, $\Gamma_m = E$, $E = \sum_m E_m$, and $\exp(t\hat{Q}) = \exp(-tE) \mathcal{G}^{(0)}(t)$, where $\mathcal{G}^{(0)}$ is the response function of an infinite, uniform chain (equation (2.14)). Finally, we restrict our discussion to the case of *shunting inhibition*, $S^{(i)} = 0$. Thus the inhibitory inputs do not contribute directly to the membrane potential $V(t)$ in equation (3.2) but affect its behaviour indirectly through the presence of the factor e^{-tE} . Taking the limit $t \rightarrow \infty$ in equation (3.2) then leads to the result that the steady-state potential V^∞ at the soma ($m = 0$) in response to constant non-recurrent lateral inhibition (figure 2) is

$$V^\infty(E) = S^{(e)} E \sum_{n \neq 0} a_n G_{0n}^{(0)}(E) \quad (3.5)$$

where $G^{(0)}$ is the Laplace transform of $\mathcal{G}^{(0)}$,

$$G_{mn}^{(0)}(E) = \int_0^\infty dt' e^{-t'E} \mathcal{G}_{mn}^{(0)}(t'). \quad (3.6)$$

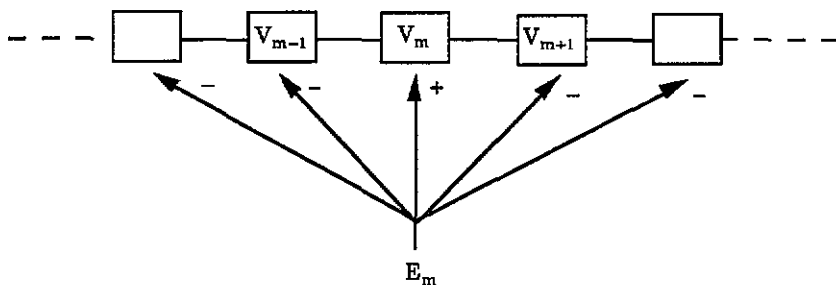


Figure 2. Pattern of excitatory and inhibitory inputs in the case of non-recurrent lateral inhibition.

Note that in the long-time limit we can neglect the effects of any transients since the matrix Q has negative definite eigenvalues.

Substituting equation (2.14) into equation (3.6) gives

$$G_{mn}^{(0)}(E) = \int_{-\pi}^{\pi} \frac{dk}{2\pi} \frac{e^{ik(n-m)}}{\epsilon(k) + E} \tag{3.7}$$

Equation (3.7) may be rewritten as a contour integral on the unit circle C in the complex plane. That is, introducing the change of variables $z = e^{ik}$ and substituting for $\epsilon(k)$ using equation (2.15),

$$G_{mn}^{(0)}(E) = \oint_C \frac{dz}{2\pi i} \frac{z^{n-m}}{(E + \tau^{-1} + 2\tau'^{-1})z - \tau'^{-1}(z^2 + 1)} \tag{3.8}$$

The demoninator in the integrand of equation (3.8) has two roots,

$$\lambda_{\pm} = 1 + \frac{\tau'(E + \tau^{-1})}{2} \pm \sqrt{\left(1 + \frac{\tau'(E + \tau^{-1})}{2}\right)^2 - 1} \tag{3.9}$$

with λ_- lying within the unit circle. Hence, evaluating equation (3.8) we obtain

$$G_{0n}^{(0)}(E) = \tau' \frac{(\lambda_-(E))^n}{\lambda_+(E) - \lambda_-(E)} \tag{3.10}$$

It follows from equations (3.10) and (3.5) that for low levels of excitation E , V^∞ is approximately a linear function of E . However, as E increases, the contribution of shunting inhibition to the effective time constant becomes more and more significant, and V^∞ eventually begins to decrease. For large E ,

$$V^\infty(E) \approx S^{(e)} E \sum_{n \neq 0} a_n (\lambda_-)^n \tag{3.11}$$

with $\lambda_- \rightarrow 0$ and hence $V^\infty(E) \rightarrow 0$ as $E \rightarrow \infty$.

Now consider a population of excitatory neurons, each of which has the pattern of stimulation as described above with the net excitatory rate E impinging on an individual neuron being determined by the average firing rate $\langle f \rangle$ of the population. For a large population, a reasonable approximation is to take $\beta E = \langle f \rangle$ for some constant β . Within

a mean field approach the steady-state behaviour is given by the self-consistency condition (Abbott 1991)

$$\beta E = F(V^\infty(E)) \quad (3.12)$$

where F is the sigmoidal function of equation (2.2) and $V^\infty(E)$ satisfies equation (3.10). Using graphical methods (Abbott 1991, Bressloff and Taylor 1993a, b) it can be shown that there are two stable solutions to equation (3.12), one corresponding to the silent state $E = 0$ and the other to a state with a firing rate well below f_{\max} . On the other hand, in the absence of shunting, $V^\infty(E)$ is a linear function of E , and the second stable state has a firing rate close to f_{\max} . Since the network settles into a state of low firing rate in the presence of shunting, one can take the output function F to be approximately linear. Such a linearization will greatly simplify our subsequent analysis.

In the above analysis, the pattern of non-recurrent inhibition (figure 2) was chosen so that the shunting term Γ_m was site-independent, allowing the Green's function $\mathcal{G}^{(0)}$ of a uniform dendritic chain to be used. We shall now consider a more general pattern of shunting inhibition, which includes synaptic background activity, and determine the resulting changes in the steady-state behaviour of the neuron population. In particular, suppose that a given neuron in the population has a pattern of input stimulation given by equation (3.4) except that there is an additional random background contribution to the inhibitory rate H_m ,

$$H_m = \sum_{n \neq m} E_n + \xi_m. \quad (3.13)$$

We shall assume that the ξ_m are distributed randomly across the population of neurons according to the probability density $\rho(\xi)$, where ρ is site-independent. (For simplicity, any correlations between ξ s at different sites are discounted, $\langle \xi_m \xi_n \rangle = 0$ for $m \neq n$.) Setting $\hat{\mathcal{G}}(t) = \mathcal{G}(t)e^{-tE}$, the steady-state membrane potential at the soma of an arbitrary neuron in the population is given by

$$V^\infty(E) = S^{(e)} E \sum_{n \neq 0} a_n G_{0n}(E) \quad (3.14)$$

where $G(E)$ is the Laplace transform of $\mathcal{G}(t)$,

$$G(E) = \int_0^\infty dt \exp(-tE) \exp[t(Q^{(0)} - \text{diag}(\xi))]. \quad (3.15)$$

Note that $\mathcal{G}(t)$ is the Green's function of a infinite, non-uniform dendritic chain where the source of non-uniformity is the random background ξ_m .

Using mean field arguments we now take E to satisfy the self-consistency condition

$$\beta E = \langle F(V^\infty(E)) \rangle_\xi. \quad (3.16)$$

The solution to this equation then determines the average firing rate of the network. The evaluation of the ensemble average over ξ in equation (3.16) is a non-trivial problem for a nonlinear function F such as a sigmoidal. However, progress can be made if we assume that the firing rate is a linear function of V^∞ (see previous comments) such that equation (3.16) is replaced by

$$\beta E = \alpha \langle V^\infty(E) \rangle_\xi + \varphi \quad (3.17)$$

for constants, α, φ . As we shall show in the next section, approximate expressions for the ensemble average of $G(E)$ can be obtained using Green's function techniques familiar from the theory of disordered crystalline solids (Elliott *et al* 1974, Ziman 1979). One particular result is that $\langle G(E) \rangle_\xi$ has the general form

$$\langle G_{mn}(E) \rangle_\xi = \int_{-\pi}^{\pi} \frac{dk}{2\pi} \frac{e^{ik(m-n)}}{\epsilon(k) + E + \Sigma(E, k)}. \tag{3.18}$$

Thus, although for the disordered system (non-zero random background activity) $G_{mn}(E)$ is not simply a function of the relative displacement $m - n$, translational invariance is recovered on performing the ensemble average over ξ . This reflects the fact the density $\rho(\xi)$ has been taken to be site-independent. Comparing equation (3.18) with equations (3.7) and (3.8) we see that the so-called 'self-energy' term $\Sigma(E, k)$ alters the pole structure in k -space and hence the value of the eigenvalues λ_\pm in equation (3.9). We shall investigate how this affects the average firing rate of the network in section 4.

4. Green's function formalism

We begin our analysis of $\langle G(E) \rangle_\xi$ by noting from equation (3.15) that $G(E)$ satisfies

$$\sum_{m'} [Q_{mm'}^{(0)} - (\xi_m + E)\delta_{mm'}] G_{m'n}(E) = -\delta_{mn} \tag{4.1}$$

where $Q^{(0)}$ satisfies equation (2.16). In other words, the Laplace-transformed Green's function $G(E)$ may be rewritten as the inverse operator

$$G(E) = [EI - Q]^{-1} \tag{4.2}$$

with $Q_{mn} = Q_{mn}^{(0)} - \xi_m \delta_{mn}$ and I the unit matrix. Furthermore, in the absence of synaptic background activity ($\xi_m \equiv 0$) one obtains

$$G^{(0)}(E) = [EI - Q^{(0)}]^{-1} \tag{4.3}$$

where $G^{(0)}(E)$ is the Laplace-transformed Green's function of a uniform chain, equation (3.7).

We deduce from equation (4.1) the following result: the (Laplace-transformed) Green's function of a uniform dendritic chain with random synaptic background activity satisfies a matrix equation identical in form to that found in the TBA model of excitations on a one-dimensional disordered lattice. In the former model, $Q^{(0)}$ represents the electrical properties of the dendritic chain, E is the total rate of input excitation and ξ is the synaptic background activity, which may be considered as a random perturbation of $Q^{(0)}$; the ensemble average $\langle G(E) \rangle$ determines the average firing rate of a population of neurons. On the other hand, in the TBA model, $Q^{(0)}$ represents an effective Hamiltonian perturbed by the diagonal disorder ξ and E is the energy of excitation; $\langle G(E) \rangle$ determines properties of the system such as the density of energy eigenstates. (For a review of TBA models, see Elliott *et al* (1974) and chapter 9 of Ziman (1979).)

The above result implies that many of the Green's function techniques developed for the evaluation of $\langle G(E) \rangle$ within the context of TBA models may be carried over to the dendritic model. As described more fully below, such techniques involve expanding $G(E)$

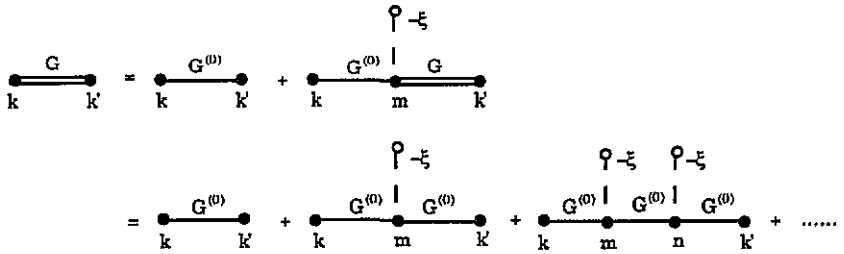


Figure 3. Diagrams appearing in the Dyson expansion of the single-neuron Green's function.

of equation (4.2) as a series in ξ , taking the ensemble average term by term, and resumming the series according to some approximation scheme; an exact resummation is not generally possible. Such a resummation leads to an approximate expression for the self-energy matrix $\Sigma(E, k)$ of equation (3.18). One condition on the validity of any approximation scheme for the dendritic model is that the resulting self-energy is positive, $\Sigma \geq 0$; this is a consequence of the fact that $\xi_m \geq 0$ for all m and all elements of the ensemble. Such a condition will also ensure that $\langle G(t) \rangle \rightarrow 0$ in the limit $t \rightarrow \infty$. One should note that although the TBA and dendritic models are formally equivalent, they describe very different physical systems. Thus, there are differences between the two models with respect to the restrictions imposed on the nature of ξ and on the interpretation of $\langle G(E) \rangle$. With this in mind, we shall now describe how the Green's function formalism of disordered systems can be applied to our neural network model. We shall follow closely the discussion of Ziman (1979), to which we refer the reader for more details.

4.1. Propagator expansion

Formal manipulation of equation (4.2) leads to the Dyson equation

$$G = G^{(0)} - G^{(0)} \Lambda G \tag{4.4}$$

where $\Lambda = \text{diag}(\xi)$. (To obtain formal equivalence with the expressions of Ziman (1979) replace ξ_m by $-\xi_m$.) Equation (4.4) may be expanded as a series in ξ such that

$$G_{kk'} = G_{kk'}^{(0)} - \sum_m G_{km}^{(0)} \xi_m G_{mk'}^{(0)} + \sum_{m,n} G_{km}^{(0)} \xi_m G_{mn}^{(0)} \xi_n G_{nk'}^{(0)} - \dots \tag{4.5}$$

Equations (4.4) and (4.5) are represented diagrammatically in figure 3. At first sight it would appear that one could determine $\langle G \rangle$ by performing an ensemble average of the right-hand side of equation (4.5) term by term. However, the resulting series cannot be resummed exactly. The simplest and crudest approximation is to replace each factor ξ_m by the site-independent average $\bar{\xi}$. This leads to the so-called *virtual crystal approximation* (VCA), where

$$\langle G(E) \rangle = G^{(0)}(E + \bar{\xi}). \tag{4.6}$$

That is, statistical fluctuations associated with the random synaptic inputs are ignored so that the ensemble-averaged Green's function is equivalent to the Green's function of a uniform dendritic chain with a modified membrane time constant such that $1/\tau \rightarrow 1/\tau + \bar{\xi}$ (see equation (3.7)).

When we attempt to take into account statistical fluctuations we run into the difficulty that there are no restrictions imposed on the summation over site indices so that an element ξ_m may appear several times in the same product. For example, if a particular term in the series expansion of equation (4.5) involves ξ_m^2 then ensemble averaging will lead to a contribution $\Delta = \langle \xi^2 \rangle$, and in general the variance of ξ will be non-zero, implying $\Delta \neq \bar{\xi}^2$. This is illustrated diagrammatically in figure 4. Thus, the ensemble average of the series will lead to successively more complex contributions from successive terms whose sum cannot be calculated exactly. Hence, various approximation schemes have been developed to improve upon the VCA formulation.

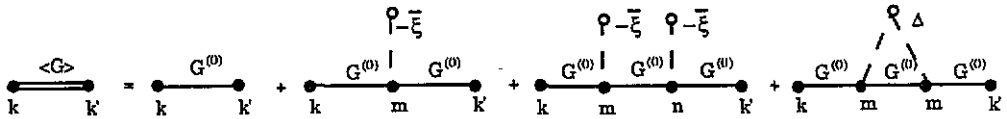


Figure 4. Diagrams appearing in the expansion of the ensemble-averaged Green's function.

One of the simplest schemes is based on a partial resummation over diagrams involving unbroken strings of repeated site indices. For example, the series in figure 5 may be summed using a Dyson equation to obtain the renormalized background contribution,

$$\eta_m = \xi_m - \xi_m G_{mm}^{(0)} \xi_m + \xi_m G_{mm}^{(0)} \xi_m G_{mm}^{(0)} \xi_m - \dots = \frac{\xi_m}{1 + \xi_m G_{00}^{(0)}}. \quad (4.7)$$

In equation (4.7) we have exploited the translational invariance of $G^{(0)}$. It follows that such diagrams can be removed from the full propagator expansion of equation (4.5) by replacing the synaptic background ξ_m with the renormalized background η_m and requiring nearest-neighbour site indices to be different,

$$G_{kk'} = G_{kk'}^{(0)} - \sum_{m \neq k, k'} G_{km}^{(0)} \eta_m G_{mk'}^{(0)} + \sum_{\substack{m \neq k, n \\ n \neq k'}} G_{km}^{(0)} \eta_m G_{mn}^{(0)} \eta_n G_{nk'}^{(0)} + \dots \quad (4.8)$$

There still remains the problem of repeated indices on non-nearest-neighbour sites. However, if an ensemble average of equation (4.8) is taken, then correlations contribute less than they do in the original series (4.5). Therefore, an improvement on the VCA is expected when η_m in equation (4.8) is replaced by the ensemble average $\bar{\eta}$, where

$$\bar{\eta} = \int \frac{\xi}{1 + \xi G_{00}^{(0)}} \rho(\xi) d\xi. \quad (4.9)$$

Note that $\bar{\eta}$ is an implicit function of E . The resulting series can be summed to obtain an approximation $\tilde{G}(E)$ to the ensemble-averaged Green's function $\langle G(E) \rangle$ given by

$$\tilde{G}(E) = G^{(0)}(E + \tilde{\Sigma}(E)) \quad (4.10)$$

where

$$\tilde{\Sigma}(E) = \frac{\bar{\eta}(E)}{1 - \bar{\eta}(E) G_{00}^{(0)}(E)}. \quad (4.11)$$

The above approximation is known in the theory of disordered systems as the *average t-matrix approximation* (ATA).

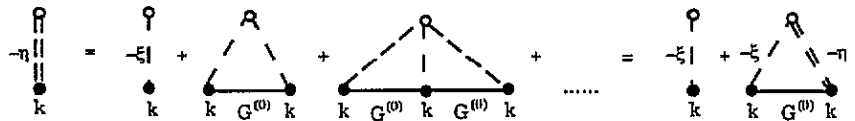


Figure 5. Diagrammatic representation of the renormalized synaptic background.

4.2. Coherent potential approximation

The most effective single-site approximation scheme in the study of disordered lattices is the so-called *coherent potential approximation* (CPA). In the context of our neural network model, this scheme involves taking each dendritic compartment to have an effective (site-independent) background synaptic input $\hat{\Sigma}(E)$ for which the associated Green’s function is

$$\hat{G}(E) = G^{(0)}(E + \hat{\Sigma}(E)). \tag{4.12}$$

The self-energy term $\hat{\Sigma}(E)$ is assumed to take account of any statistical fluctuations (at least at the single-site level), which leads to a self-consistency condition for $\hat{\Sigma}(E)$. First, observe that $\hat{G}(E)$ satisfies a Dyson equation,

$$\hat{G} = G^{(0)} - G^{(0)} \text{diag}(\hat{\Sigma}) \hat{G}. \tag{4.13}$$

On the other hand, the true Green’s function satisfies equation (4.4). Solving equation (4.13) for $G^{(0)}$ and substituting into equation (4.4) gives

$$G = \hat{G} - \hat{G} \text{diag}(\xi - \hat{\Sigma}) G. \tag{4.14}$$

We can now analyse equation (4.14) along identical lines to the ATA scheme of the previous section. In particular, we introduce a renormalized background field

$$\hat{\eta}_m = \frac{\hat{\xi}_m}{1 + \hat{\xi}_m \hat{G}_{00}} \quad \hat{\xi}_m = \xi_m - \hat{\Sigma}(E) \tag{4.15}$$

and perform a series expansion of the form (4.8) with $G^{(0)}$ replaced by \hat{G} and η by $\hat{\eta}$. Since the self-energy term $\hat{\Sigma}(E)$ is supposed to take care of any statistical fluctuations, we should recover \hat{G} on performing an ensemble average of this series. Ignoring multi-site correlations this leads to the self-consistency condition

$$\langle \hat{\eta}_m \rangle \equiv \int \frac{\xi_m - \hat{\Sigma}(E)}{1 + (\xi_m - \hat{\Sigma}(E)) G_{00}^{(0)}(E + \hat{\Sigma}(E))} \rho(\xi) d\xi = 0. \tag{4.16}$$

This is an implicit equation for $\hat{\Sigma}(E)$ that can be solved numerically to obtain $\hat{\Sigma}(E)$ as a function of E .

A particularly simple choice for the distribution of the random background activity is to assume that each dendritic compartment receives either an input ξ_A with probability p_A or an input ξ_B with probability $p_B = 1 - p_A$. Then equation (4.16) reduces to the algebraic equation

$$\frac{p_A(\xi_A - \hat{\Sigma})}{1 + (\xi_A - \hat{\Sigma}) \hat{G}_{00}} + \frac{p_B(\xi_B - \hat{\Sigma})}{1 + (\xi_B - \hat{\Sigma}) \hat{G}_{00}} = 0. \tag{4.17}$$

It is useful to rewrite equation (4.17) in the form

$$\hat{\Sigma} = \frac{\bar{\xi} + \xi_A \xi_B \hat{G}_{00}}{1 + (\xi_A + \xi_B - \hat{\Sigma}) \hat{G}_{00}} \quad (4.18)$$

which can be evaluated by iterative substitution in the denominator. One of the important features of the CPA scheme is that it interpolates smoothly between the limits of weak and strong disorder where explicit expressions for $\hat{\Sigma}(E)$ can be obtained. The degree of disorder is measured by the ratio

$$\delta = \frac{|\xi_A - \xi_B|}{4\tau'^{-1}}. \quad (4.19)$$

The denominator in equation (4.19) is the variation of $\epsilon(k)$, equation (2.15), over the interval $-\pi \leq k \leq \pi$. In the weak disorder limit, equation (4.18) reduces to

$$\hat{\Sigma} \approx p_A \xi_A + p_B \xi_B \quad (4.20)$$

which is the result that would have been obtained using a VCA. The next order approximation to equation (4.18) is

$$\hat{\Sigma} \approx p_A \xi_A + p_B \xi_B - p_A p_B (\xi_A - \xi_B)^2 G_{00}^{(0)}. \quad (4.21)$$

On the other hand, in the case of strong disorder, $\hat{G}_{00}(E) \approx (E + \hat{\Sigma}(E))^{-1}$, which substituted into equation (4.18) leads to the result

$$\hat{G}(E) \approx p_A G^{(0)}(E + \xi_A) + p_B G^{(0)}(E + \xi_B). \quad (4.22)$$

That is, the system behaves as if there are two independent uniform dendritic chains, one with constant background ξ_A and the other with constant background ξ_B .

4.3. Analysis of network behaviour

The steady-state behaviour of our model network can be obtained quite simply in the CPA (or ATA) scheme. First the self-energy $\hat{\Sigma}(E)$ is calculated using equation (4.16) for some given density $\rho(\xi)$. Then $\hat{G}(E)$ is evaluated using equations (4.12) and (3.10), that is,

$$\hat{G}_{0n}(E) = \tau' \frac{\hat{\lambda}_-(E)^n}{\hat{\lambda}_+(E) - \hat{\lambda}_-(E)} \quad (4.23)$$

where

$$\hat{\lambda}_{\pm}(E) = 1 + \frac{\tau'(E + \hat{\Sigma}(E) + \tau^{-1})}{2} \pm \sqrt{\left(1 + \frac{\tau'(E + \hat{\Sigma}(E) + \tau^{-1})}{2}\right)^2 - 1}. \quad (4.24)$$

Finally, the steady state membrane potential at the soma averaged over all elements of the network is given by

$$\langle V^\infty(E) \rangle = S^{(e)} E \sum_{n \neq 0} a_n \hat{G}_{0n}(E). \quad (4.25)$$

To investigate the effectiveness of the CPA in determining the influence of synaptic background activity, we consider the simple Bernoulli distribution introduced at the end of section 4.2 in which $\xi_n = \xi_{A,B}$ with probability $p_{A,B}$ where n is the compartment label. For simplicity, we set $\tau = \tau'$ and $a_n = \delta_{n,1}$, i.e. excitatory inputs only impinge on the compartment at $n = 1$. We compare the results for $\langle V^\infty \rangle$ based on CPA calculations with numerical estimates. The latter are obtained by numerically solving the underlying set of differential equations (2.1) for a uniform dendritic chain of 61 compartments ($n = 0, \pm 1, \dots, \pm 30$) and averaging the steady-state membrane potential at the soma ($n = 0$) over 1000 trials. In figure 6, the average steady state $\langle V^\infty \rangle$ (in units of $S^{(e)}$) is plotted as a function of the rate of excitation E (in units of τ) for $\xi_A = 2.0$, $\xi_B = 0.0$ and $p_{A,B} = \frac{1}{2}$; the degree of disorder is low with $\delta = 0.5$. The data points are based on numerical estimates whereas curve (ii) is based on CPA calculations. Curve (i) corresponds to zero background activity. The analogous results for $\xi_A = 10.0$, $\xi_B = 0.0$ and $p_{A,B} = \frac{1}{2}$ are displayed in figure 7. Here, the degree of disorder is relatively large with $\delta = 2.5$. It can be seen that good agreement between theoretical and numerical estimates are obtained in both cases.

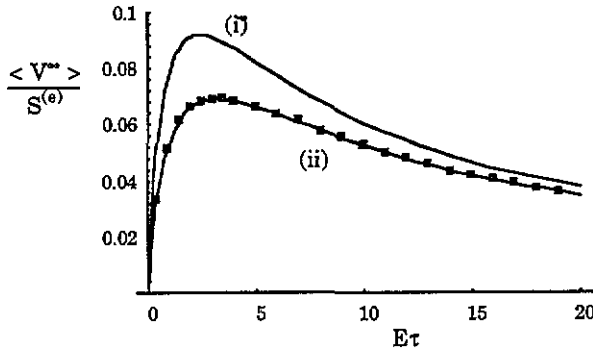


Figure 6. Expectation value of the steady-state membrane potential $\langle V^\infty \rangle$ (in units of $S^{(e)}$) as a function of the net rate of excitation E (in units of τ). Data points are obtained from numerical estimates of $\langle V^\infty \rangle$ for a non-zero synaptic background with $\xi_A = 2.0$, $\xi_B = 0.0$ and $p_{A,B} = \frac{1}{2}$. Curve (ii) represents the corresponding values for $\langle V^\infty \rangle$ calculated using the CPA. Curve (i) shows the membrane potential in the absence of a random background.

Having determined the average steady state $\langle V^\infty \rangle$, the firing rate of the network can then be found by solving the mean field equation (3.17). We shall proceed within the CPA scheme. Substituting equation (4.25) into equation (3.17) with $a_n = \delta_{n,1}$ gives

$$\beta E = \alpha S^{(e)} E G_{01}^{(0)}(E + \hat{\Sigma}(E)) + \varphi \quad (4.26)$$

where $\hat{\Sigma}(E)$ satisfies equation (4.18). It is useful to consider the solutions to equation (4.26) from a graphical viewpoint. In terms of figure 6 or 7, these solutions correspond to the points of intersection of the straight line $(\beta E - \varphi)/\alpha S^{(e)}$ with curve (ii), which is the CPA-based calculation of $\langle V^\infty \rangle / S^{(e)}$. It is clear that there are two points of intersection, one on either side of the peak of curve (ii). However, the only one of interest is located on the portion of the curve with negative slope, since it may be identified with the state of low firing discussed in section 3. One can show this by considering the corresponding solutions

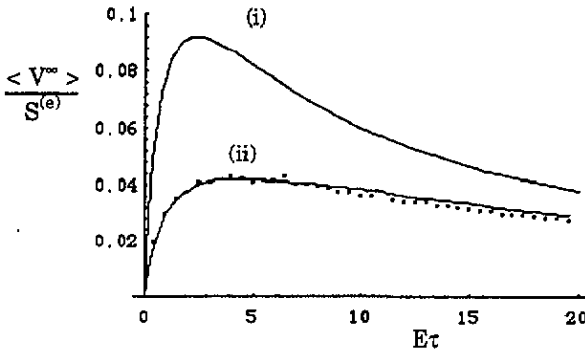


Figure 7. Same as figure 6 with $\xi_A = 10.0$, and $\xi_B = 0.0$.

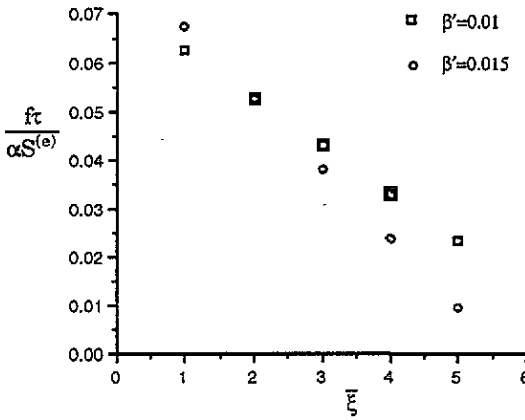


Figure 8. Firing rate f (in units of τ^{-1}) as a function of the mean level of background activity for fixed variance ($\sigma^2 = 1$).

in the case of zero background activity and nonlinear response function F (equation (2.2)) (Bressloff and Taylor 1993a, b).

The required solution, which is denoted by E^* , may be obtained by numerically solving the simultaneous equations (4.26) and (4.18). The results are displayed in figures 8 and 9, where the steady-state firing-rate f , $f = \beta E^*$, is plotted for a range $\xi_{A,B}$ values. The firing rate and the inputs E^* , $\xi_{A,B}$ are all measured in units of $1/\tau$, and the constant φ is set to zero for simplicity. Two particular cases are considered. The first is the variation of f with the mean $\bar{\xi} = p_A \xi_A + p_B \xi_B$ for fixed variance $\sigma^2 = p_A p_B (\xi_A - \xi_B)^2$, as shown in figure 8 for $\beta' = 0.01$ and $\beta' = 0.015$, where $\beta' = \beta / \alpha S^{(e)}$. It can be seen that the firing rate decreases as the mean activity across the network increases. The second case is the variation of f as a function of σ^2 for fixed $\bar{\xi}$. Here the firing rate increases as the variance in the distribution of activity across the network increases (see figure 9). In the low-disorder limit, the dependence on $\bar{\xi}$ and σ^2 can be deduced immediately from equation (4.21), after rewriting it in the form $\hat{\Sigma}(E) \approx \bar{\xi} - \sigma^2 G_{00}^{(0)}(E)$.

We conclude from the above results that (i) synaptic background activity can influence the behaviour of a neural network and, in particular, leads to a reduction in the steady-state firing rate of a network, and (ii) a uniform background reduces the firing rate more than a

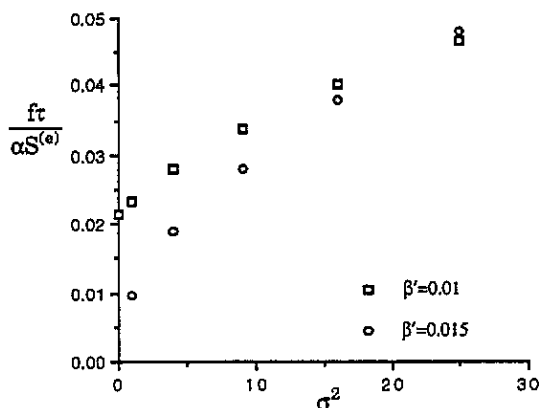


Figure 9. Firing rate as a function of the background variance at a fixed level of mean activity ($\bar{\xi} = 1$).

randomly distributed background. Note that the former result is independent of the choice of distribution ρ of ξ (discrete or continuous) since synaptic background activity can only produce a positive self-energy term $\hat{\Sigma}$, i.e. $\xi \geq 0$, and $\hat{G}(E) \equiv G^{(0)}(E + \hat{\Sigma}(E)) < G^{(0)}(E)$ for $\hat{\Sigma} > 0$. It is unclear whether or not the latter result also extends to arbitrary positive distributions ρ . We hope to consider this issue further elsewhere.

5. Discussion

The main theme of this paper has been that random synaptic background activity can lead to non-trivial changes in the steady-state behaviour of a shunting neural network. This was demonstrated within a mean field theory framework by considering the states of self-sustained firing in a recurrent network. It was shown how the effects of a random background could be taken into account using Green's function techniques developed originally for the study of excitations on disordered lattices. A general result of this paper is that background synaptic activity reduces the steady-state firing rate of a network. If the background is distributed according to a Bernoulli distribution, then we have the further result that a uniform background leads to a greater reduction in the firing rate than a randomly distributed background. A few comments are in order:

(a) A major simplification of our analysis is to take the firing rate to be a linear function of the membrane potential of a neuron. A partial justification of this is that, in the absence of background activity, the network settles into a state that has a relatively low firing rate, i.e. the neurons operate in the linear regime of the sigmoid function F (equation (2.2)). A fuller treatment would need to evaluate ensemble averages of the form $\langle F(V^\infty) \rangle_\xi$. One approach might be to perform a perturbation expansion in the gain function g leading to higher-order terms such as $\langle G(E)G(E) \rangle_\xi$; these can then be evaluated using an extension of the Green's function techniques presented in this paper (see Elliott *et al* 1974).

(b) Another possible application of the Green's function formalism is analysing the linear frequency response of a population of lateral inhibitory networks in the presence of random synaptic background activity. Lateral inhibitory networks play an important role in both the visual (Hartline 1974) and auditory systems (Shamma 1989). A major difference between this problem and the one considered in the present paper is that the former is

concerned with Fourier rather than Laplace transforms, i.e. E is replaced by $i\omega$ where ω is the frequency of response. It follows that the self-energy term Σ becomes complex, leading to a non-trivial modification in both the phase and amplitude of the average response.

References

- Abbot L F 1991 Realistic synaptic inputs for model neural networks *Network* **2** 245–58
- Amit D J 1989 *Modelling Brain Function* (Cambridge: Cambridge University Press)
- Amit D J and Treves A 1989 Associative memory neural networks with low temporal spiking-rates *Proc. Natl Acad. Sci. USA* **86** 7671
- Bernander O, Douglas R J, Martin A C and Koch C 1991 Synaptic background activity influences spatiotemporal integration in single pyramidal cells *Proc. Natl Acad. Sci. USA* **88** 11 569–73
- Bressloff P C 1993 Temporal processing: a compartmental approach *Network* **4** 155
- Bressloff P C and Taylor J G 1993a Low firing-rates in a compartmental model neuron *J. Phys. A: Math. Gen.* **26** L165
- 1993b Spatio-temporal pattern processing in a compartmental model neuron *Phys. Rev. E* **47** 2899
- 1993c Compartmental model response function for dendritic trees *Biol. Cybern.* **70** 199
- Elliott R J, Krumhansl J A and Leath P L 1974 The theory and properties of randomly disordered crystals and related physical systems *Rev. Mod. Phys.* **46** 465
- Hartline H K 1974 *Studies on Excitation and Inhibition in the Retina* ed E Ratliff (New York: Rockefeller University Press)
- Perkel D H, Mulloney B and Budelli R W 1981 Quantitative methods for predicting neuronal behaviour *Neuroscience* **6** 823–37
- Rall W 1964 *Neural Theory and Modeling* ed R F Reiss (Stanford: Stanford University Press) pp 73–97
- 1967 Distinguishing theoretical synaptic potentials computed for different soma-dendritic distributions of synaptic inputs *J. Neurophys.* **30** 1138–68
- Rapp M, Yarom Y and Segev I 1992 The impact of parallel fiber background activity on the cable properties of cerebellar Purkinje cells *Neural Comput.* **4** 518–33
- Rubin N and Sompolinsky H 1989 Neural networks with low firing-rates *Europhys. Lett.* **10** 465
- Shamma S 1989 *Methods in Neuronal Modelling* ed C Koch and I Segev (Cambridge, MA: MIT Press) pp 247–89
- Ziman J M 1979 *Models of Disorder* (Cambridge: Cambridge University Press)